Optical and thermal properties of fibres: effect of boiling and stretching on some macro-structural parameters of polyester fibres

1999 J. Phys.: Condens. Matter 11 3371

(http://iopscience.iop.org/0953-8984/11/16/017)

J. Phys.: Condens. Matter **11** (1999) 3371–3385. Printed in the UK PII: S0953-8984(99)97000-5

Optical and thermal properties of fibres: effect of boiling and stretching on some macro-structural parameters of polyester fibres

I M Fouda† and H M Shabana
Department of Physics, Faculty of Science, University of Mansoura, Mansoura 35516, Egypt

Received 26 August 1998, in final form 27 January 1999

Abstract. Unboiled and boiled polyester (PET) (Egyptian manufacturer) fibres having irregular cross-sectional shape were stretched at room temperature using a mechanical device with a double-beam interference microscope. The optical results obtained were used for calculating some macro-structural parameters. The evaluated density results were used to calculate the degree of crystallinity, the form birefringence, the mean square density fluctuation and some other macro-structural parameters at different stresses and different boiling times. Relationships between the macro-structural parameters with different stresses are given for these fibres. The investigated parameters changed with boiling and stretching. So the obtained results clarify that reorientation occurred. Empirical formulae were suggested to correlate the changes in some structural parameters with different draw ratios, and their constants were determined. This means that the series and parallel components are deformed in the same mode by drawing.

1. Introduction

Oriented polymers have birefringence: the refractive indices along the orientation and at right angle to it are different. When this difference (Δn) is larger, the segments are oriented more in the direction of force action. The refractive indices of fibres indicate the molecular packing density of the fibres along the directions.

Optical anisotropy produced in fibres gives valuable information for characterization of these fibres on the molecular level and various processes have been used and developed for this purpose. Optical anisotropy changes the random molecular orientation of the isotropic polymers. The orientation can be produced by either hot stretching of a molten polymer followed by rapidly cooling of the melt, or by cold drawing or by cold rolling. The degree of orientation could vary significantly from one fibre to another depending on the fibre history during manufacturer and subsequent processing operations. The strain hardening generally results from molecular orientation which increases the modulus, and tensile strength [1–8].

Poly(ethylene terephthalate) provides a very good mouldable, film forming and fibre forming polyester because of its high glass transition temperature (70–80 °C) and high crystalline melting point (>250 °C). Poly(ethylene terephthalate) (PET) fibres are among the most important synthetic fibres. Several investigations have been made for developing the molecular orientation in PET fibres [9–18].

† Corresponding author. E-mail address: sinfac@mum.mans.eun.eg.

0953-8984/99/163371+15$19.50

In the present work a modified micro-strain device [19, 20] is used in conjunction with a Pluta polarizing interference microscope to study some structural parameters produced in boiled PET fibres. The variations of refractive indices and birefringence by different stresses were studied previously by Fouda and Shabana [21]. The resulting data are utilized to calculate the orientation functions and the isotropic refractive index by Lorentz–Lorenz equation. Also calculations of the harmonic mean polarizability of the dielectric, the harmonic mean specific refractivity, the number of the monomeric units per unit volume, the electric polarizability polymer structure constant $(\Delta\tau/3\tau_0)$ and some other structural parameters are given.

2. Theoretical consideration

The refractive indices and birefringence of PET fibres having irregular cross-sectional shape are measured by a double-beam interference Pluta microscope [21–23]. The values obtained for $n^{\parallel}$, $n^{\perp}$ and Δn are utilized for calculating some optical and structural parameters. The optical orientation function f_{Δ} was calculated by Hermans [24] and Ward [25, 26] from the following equation

$$f_{\Delta} = \frac{\Delta n}{(\Delta n)_{max}} = \langle P_2(\theta)\rangle \tag{1}$$

where $(\Delta n)_{max}$ is the maximum birefringence of a fully oriented fibre. Its value has been previously [24] determined to be 0.24 for PET. $\langle P_2(\theta)\rangle$ is related to the polarizabilities $\Phi^{\parallel}$ and $\Phi^{\perp}$ by the relation [27]

$$\frac{\Phi^{\parallel} - \Phi^{\perp}}{\Phi^{\parallel} + 2\Phi^{\perp}} = \langle P_2(\theta)\rangle P_2(\theta_m) \tag{2}$$

where $P_2(\theta_m)$ is constant. The values of $\Phi^{\parallel}$, $\Phi^{\perp}$ are determined from the following equation due to Stein and Wilkes [28]

$$\Phi^{\parallel} = \frac{n_{\parallel}^2 - 1}{n_{\parallel}^2 + 2}. \tag{3}$$

Equation (2) can be written in the form

$$\frac{\Phi^{\parallel} - \Phi^{\perp}}{\Phi^{\parallel} + 2\Phi^{\perp}} = \left[\frac{\Delta\tau}{3\tau_0}\right]\langle P_2(\theta)\rangle \tag{4}$$

where $(\Delta\tau/3\tau_0)$ is a quantity depending on the molecular structure, and can be obtained from the relation between $P_2(\theta)$ and $[(\Phi^{\parallel} - \Phi^{\perp})/(\Phi^{\parallel} + 2\Phi^{\perp})]$.

The function f_{θ} is developed in an approach to the continuum theory of birefringence of oriented polymer [29] where

$$f_{\theta} = \frac{n_1^2 n_2^2}{n_{\parallel}^2 + n_{\perp}^2}\frac{n_{\parallel} + n_{\perp}}{n_1 + n_2}\frac{\Delta n}{\Delta n_{max}}. \tag{5}$$

n_1 and n_2 were previously determined [29] to be 1.815 and 1.575, respectively. Equation (5) is slightly different from the original expression in equation (1), used by Hermans and Platzek [30] and Kratky [31], can be given by the following equation

$$f_{\theta} = (1 + a) f_{\Delta} - a f_{\Delta}^2. \tag{6}$$

The value of a constant a was calculated to be 0.2. The angle θ is determined from the following equation [24]:

$$f_{\theta} = 1 - \tfrac{3}{2}\sin^2\theta \tag{7}$$

and analogous equation for f_Δ and θ'.

For random links, the orientation function $P_2(\theta)$ as previously calculated [15] is given by

$$P_2(\theta) = (D^2 - D^{-1})/5N_1 \tag{8}$$

where N_1 is defined as the number of random links between the network junction points (the entanglements).

Roe and Krigbaum [32] derived an expression for the distribution function of segments at an angle θ with respect to the draw ratios.

$$\omega(\cos\theta) = \frac{1}{2} + \frac{1}{4N_1}(3\cos^2\theta - 1)(D^2 - D^{-1}). \tag{9}$$

Before orientation, the segments will be randomly oriented at an angle θ with respect to the draw direction. After drawing the segments will be constrained at an angle β given by

$$\tan\beta = D^{-3/2}\tan\theta. \tag{10}$$

2.1. Form birefringence [7]

Form birefringence is a phenomenon that is found in materials having two or more separate phases with different refractive indices and obtained by the following equation [7]

$$\Delta n = \chi_c \Delta n_c + (1 - \chi_c)\Delta n_a + \Delta n_f \tag{11}$$

where Δn_c = the birefringence per unit volume for crystalline polymer and Δn_a = the birefringence per unit volume for amorphous polymer and χ_c the volume fraction of crystalline regions. The values of Δn_c and Δn_a equal 0.22 and 0.27 for PET, respectively [7].

The densities of PET samples are estimated with the average refractive indices obtained by the two-beam interferometric technique from the following relation [33]:

$$\rho = 4.047\frac{(\bar{n}^2 - 1)}{(\bar{n}^2 + 2)} \tag{12}$$

with ρ expressed in kg cm^{-3}. We calculate $\bar{n}$ as the isotropic refractive index.

2.2. Crystallinity evaluation from density values [34]

The degree of crystallinity, χ, is determined by the relation

$$\chi = \frac{\rho - \rho_a}{\rho_c - \rho_a} \tag{13}$$

where ρ_c and ρ_a are the densities of the crystalline and non-crystalline [35] regions, with $\rho_c = 1.457$ g cm^{-3} and $\rho_a = 1.336$ g cm^{-3}.

For a two-phase structure consisting of amorphous and crystalline regions with densities ρ_c and ρ_a, respectively, the mean square density fluctuation $\langle\eta^2\rangle$ can be calculated from the following equation [36]

$$\langle\eta^2\rangle = (\rho_c - \rho_a)^2\chi(1 - \chi). \tag{14}$$

2.3. Calculation of the isotropic refractive index from the Lorentz–Lorenz equation

The Lorentz–Lorenz equation is used to correlate the polarizabilities and refractive index, including the density parameters, as follows [37]

$$\frac{n^2_{iso(2)} - 1}{n^2_{iso(2)} + 2} = \frac{1}{3}\frac{\rho_i}{\rho}\left[\frac{n^2_\parallel - 1}{n^2_\parallel + 2} + 2\frac{n^2_\perp - 1}{n^2_\perp + 2}\right] \tag{15}$$

where ρ and ρ_i are the densities of the evaluated and of the isotropic tested polymer, respectively, and $\rho_i = \rho_a = 1.336$ cm^{-3}.

2.4. Mean polarizability of monomer unit

For a bulk polymer of density ρ and monomer unit molecular weight M, the number of monomer units per unit volume $N_m = N_a\rho/M$ where N_A is Avogadro's number 6.02×10^{23} mol^{-1} and M for PET = 192 [29].

As the refractive index of a polymer depends on the total polarizability of the molecules, this leads to the Lorentz–Lorenz equation by the following equations [38]:

$$\frac{n_\parallel^2 - 1}{n_\parallel^2 + 2} = \frac{N_m \alpha^\parallel}{3\Psi_0} \tag{16}$$

with an analogous formula used for $n_\perp$ and $\bar{n}$, where $n_\parallel$ and $n_\perp$ are the mean refractive indices of the fibre for light vibrating along and across the fibre axis. $\bar{n}$ is the average refractive index (isotropic refractive index), $\alpha^\parallel$ is the mean polarizability of the dielectric and Ψ_0 is the permittivity of free space $= 8.85 \times 10^{-12}$ F m^{-1}. The left-hand side of equation (16) is proportional to the density ρ (kg m^{-3}) of the medium and may also be written in the form, given by De Vries [29],

$$\frac{n^2 - 1}{n^2 + 2} = \frac{N_m \alpha}{3\Psi_0} = \varepsilon\rho \tag{17}$$

where ε (m^3 kg^{-1}) is called the specific refractivity of the isotropic dielectric.

2.5. Calculation of the molar refractivity [39]

The polarizability of a molecule is related to its refractive index by the Lorentz–Lorenz relations

$$\frac{\bar{n}^2 - 1}{\bar{n}^2 + 2}\frac{M}{\rho} = 4/3\pi N_A \alpha = R \tag{18}$$

where n is the isotropic refractive index, ρ is the density, M is the molecular weight, N_A is Avogadro's number, α is the polarizability and R is the molecular or molar refractivity. The value M used is that of the repeat unit of the molecule.

3. Experimental results

3.1. Application of two-beam interferometry

PET fibres, unboiled and boiled for 30 min, 60 min and 90 min were stored after boiling in a desiccator for 24 hours. Then, they were drawn to different draw ratios up to 1.3 and examined by the double-beam interference Pluta microscope. Figures 1(a) and (b) are the obtained interferograms of two-beam interferometry from the totally duplicated image position. Plane polarized light of $\lambda = 546$ nm vibrating along and across the fibre axis, and liquid of refractive index $n_L = 1.601$ at 180 °C, is used. The corresponding draw ratios are 1 and 1.3 for the sample boiled for 60 min The values of $n^\parallel$ and $n^\perp$ are as previously obtained [21]. The results are given in table 1.

Evaluation of some structural parameters such as form birefringence Δn_f, $n_{iso(2)}$, fibre density (ρ) and crystallinity (χ) were calculated from equations (11), (15), (12) and (13), respectively. The resultant data of these parameters are given in table 1. The density increase as shown is the result of denser molecular packing from drawing induced orientation and crystallization. As the draw ratio increases the crystallinity increases, i.e, the amorphous regions decrease, which has practical importance in studying the nature of swelling and diffusion of dyes. Determination of the form birefringence arises from calculating the volume

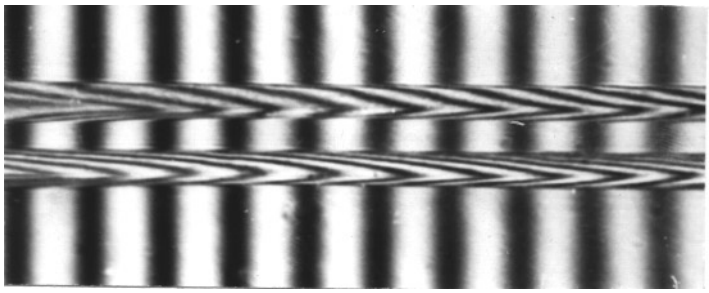

(a)

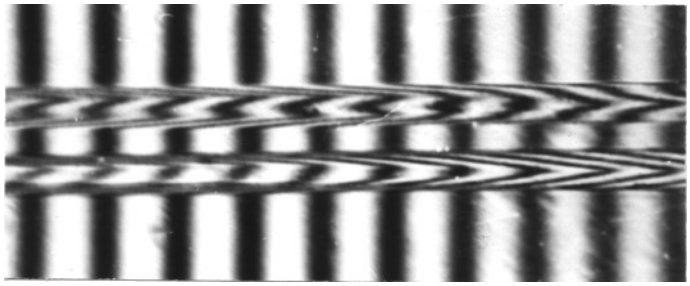

(b)

Figure 1. (a)(b) Microinterferograms of two-beam interferometry from the totally duplicated image position.

fraction of crystalline and amorphous regions in addition to the total birefringence. The form birefringence cannot be neglected and must be considered to throw light on the phase boundary between the amorphous and crystalline regions.

Figure 2 shows the relationship between the draw ratio and the crystallinity (χ) for the sample boiled for 60 min The same behaviour is found with slight differences for the other samples, see table 1.

From the resulting values of Δn the optical orientation functions $P_2(\theta)$ were calculated from equation (1) for all samples. Figure 3 shows the relationship between the orientation function $P_2(\theta)$ and the factor $(\Phi_\parallel - \Phi_\perp)/(\Phi_\parallel + 2\Phi_\perp)$ for the unboiled sample. The same behaviour is found for the other samples. The value of $(\Delta\tau/3\tau_0)$ was calculated and found to be constant, equal to 0.106 for PET, where it depends on the molecular structure. The electric polarizability constant is unaffected by both the draw ratios and the boiling times.

Also, the values of f_θ were determined by the new approach and the optical orientation angle θ, the angle between the fibre axis and the axis of the polymer units, was measured from equations (6) and (7) respectively, for all samples and is given also in table 2. The relationships between the draw ratio and both the optical orientation function f_θ and angle θ for all samples are given in figures 4(a)–(d) and 5(a)–(d). Figure 6 shows the relationship between the optical orientation function f_θ and the birefringence for the unboiled sample. The same behaviour is found with small differences for the other samples, see table 2. The number of random links N_1 between entanglements was calculated from equation (8). In addition, the distribution function of segments $\omega(\cos\theta)$ at an angle θ was determined with respect to the draw ratio from equation (9). The angle β, where the segment is constrained after drawing, is determined from equation (10). The values of N_1, $\omega(\cos\theta)$ and the angle β for all samples are also given

Table 1. Values of refractive indices, total birefringence, form birefringence, isotropic refractive index, density and crystallinity.

D	$n_a^{\parallel}$	$n_a^{\perp}$	Δn_a $\times 10^{-3}$	Δn_f $\times 10^{-3}$	$n_{iso(2)}$	ρ	χ (%)
Unboiled sample							
1	1.6721	1.5522	120	−0.136	1.5910	1.3699	28.01
1.05	1.6778	1.5496	128	−0.128	1.5913	1.3701	28.18
1.1	1.6820	1.5473	135	−0.121	1.5912	1.3699	28.01
1.15	1.6850	1.5460	139	−0.117	1.5913	1.3701	28.18
1.2	1.6885	1.5445	144	−0.112	1.5914	1.3705	28.51
1.25	1.6909	1.5433	147	−0.109	1.5917	1.3705	28.51
1.3	1.6935	1.5422	151	−0.105	1.5919	1.3706	28.60
Sample boiled for 30 min							
1	1.6735	1.5515	122	−0.134	1.5910	1.3697	27.85
1.05	1.6798	1.5496	131	−0.125	1.5914	1.3701	28.18
1.1	1.6825	1.5470	133	−0.123	1.5914	1.3697	27.85
1.15	1.6860	1.5457	140	−0.116	1.5916	1.3703	28.34
1.2	1.6892	1.5442	145	−0.111	1.5916	1.3705	28.51
1.25	1.6920	1.5430	149	−0.107	1.5917	1.3706	28.60
1.3	1.6941	1.5420	152	−0104	1.5918	1.3708	28.80
Sample boiled for 60 min							
1	1.6750	1.5512	124	−0.132	1.5911	1.3703	28.34
1.05	1.6805	1.5484	132	−0.124	1.5912	1.3703	28.34
1.1	1.6830	1.5470	136	−0.120	1.5914	1.3705	28.51
1.15	1.6870	1.5455	141	−0.115	1.5914	1.3706	28.60
1.2	1.6905	1.5438	146	−0.109	1.5915	1.3708	28.80
1.25	1.6927	1.5429	150	−0.106	1.5916	1.3710	28.90
1.3	1.6945	1.5418	153	−0.103	1.5918	1.3708	28.90
Sample boiled for 90 min							
1	1.6756	1.5510	125	−0.131	1.5911	1.3705	28.51
1.05	1.6812	1.5483	133	−0.123	1.5914	1.3706	28.60
1.1	1.6835	1.5469	138	−0.118	1.5914	1.3705	28.51
1.15	1.6875	1.5454	142	−0.113	1.5915	1.3708	28.80
1.2	1.6910	1.5436	147	−0.108	1.5916	1.3708	28.80
1.25	1.6930	1.5428	150	−0.106	1.5916	1.3710	28.90
1.3	1.6952	1.5417	153	−0.102	1.5918	1.3711	29.01

in table 2. The relationship between $\omega(\cos\theta)$ and $(D^2 - D^{-1})$ is drawn in figure 7 for the examined PET fibres.

In addition to the above structural parameters, the polarizability of a monomer unit $\alpha^{\parallel}$, $\alpha^{\perp}$ and $\bar{\alpha}$ and the specific refractivity of the isotropic dielectric $\varepsilon^{\parallel}$, $\varepsilon^{\perp}$ and $\bar{\varepsilon}$ are calculated from equations (16) and (17). The obtained values of these parameters are given in table 3. Figures 8(a) and (b) give the relationship between the draw ratios and both the mean polarizability of a monomer unit and the mean specific refractivity of the isotropic dielectric.

The mean square density fluctuation η^2, the molar refractivity R and the number of monomer units per unit volume N_m were calculated and are given in table 4. An empirical formula was suggested to evaluate the relationship between draw ratio and f_θ, $\omega(\cos\theta)$, $\varepsilon^{\parallel}$ and θ for the unboiled sample as follows:

$$\ln \frac{f_\theta \omega(\cos\theta)\varepsilon^{\parallel}}{\theta} = X_1 D + Y_1 \tag{19}$$

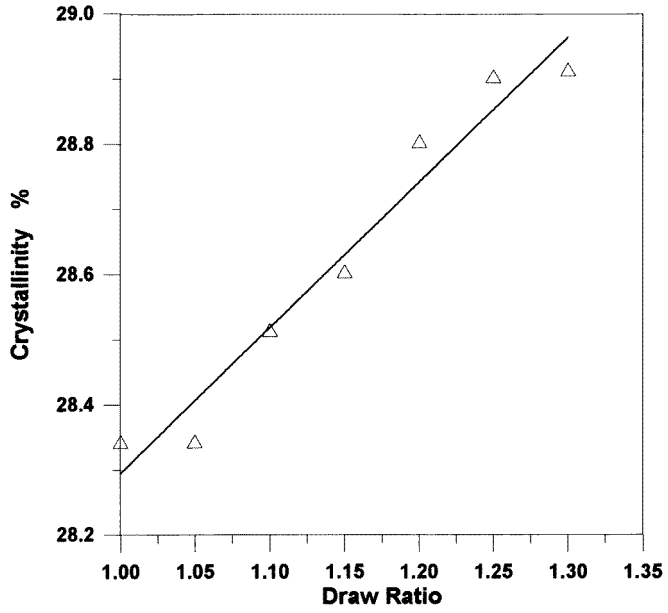

Figure 2. The relationship between the draw ratio and the crystallinity (χ).

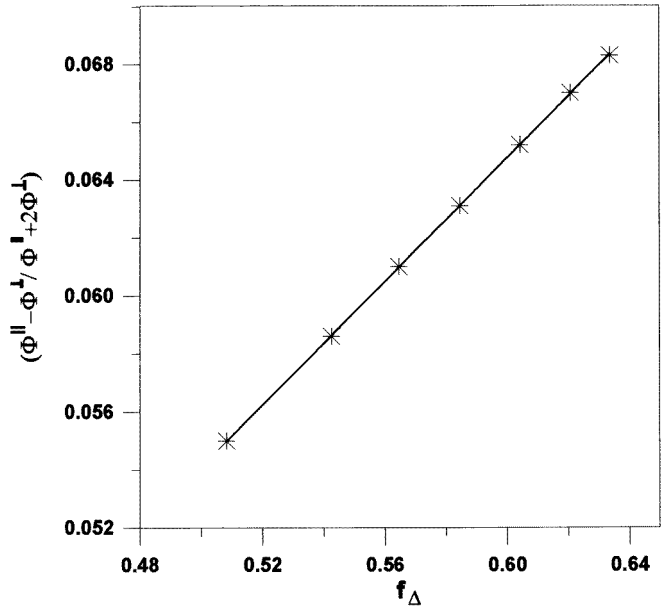

Figure 3. The relationship between the orientation function $P_2(\theta)$ and the factor $(\Phi_\parallel - \Phi_\perp)/(\Phi_\parallel + 2\Phi_\perp)$.

where X_1 and Y_1 are constants characterizing the proportionality in equation (19). The values of X_1 and Y_1 were determined to be 1.7 and -9.75, respectively (see figure 9). In a previous

Table 2. Values of f_Δ, f_θ, θ, θ', $\omega(\cos\theta)$, the angle β and the number of network junction points N_1.

D	$f_\Delta \times 10^{-3}$	$f_\theta \times 10^{-3}$	θ (°)	θ' (°)	$\omega(\cos\theta)$	β (°)	N_1
Unboiled sample							
1	499	576	35.28	32.10	0.5	32.1	—
1.05	534	615	33.86	30.44	1.32	28.6	0.056
1.1	561	645	32.74	29.11	1.41	25.7	0.106
1.15	579	665	31.98	28.21	1.46	23.5	0.155
1.2	600	687	31.09	27.15	1.53	21.3	0.200
1.25	615	704	30.44	26.37	1.58	19.5	0.247
1.3	630	721	29.76	25.55	1.64	17.8	0.290
Sample boiled for 30 min							
1	508	586	34.93	31.68	0.5	31.6	—
1.05	542	623	33.52	30.07	1.35	28.3	0.055
1.1	564	649	32.59	28.94	1.42	25.5	0.106
1.15	584	670	31.75	27.95	1.48	23.3	0.154
1.2	604	692	30.9	26.94	1.55	21.1	0.198
1.25	620	710	30.18	26.07	1.60	19.3	0.245
1.3	633	724	29.61	25.38	1.65	17.7	0.290
Sample boiled for 60 min							
1	516	594	34.62	31.34	0.5	31.2	—
1.05	550	633	33.19	29.66	1.38	27.8	0.054
1.1	567	651	32.51	28.84	1.42	25.5	0.106
1.15	589	676	31.54	27.70	1.49	23.0	0.153
1.2	611	699	30.60	26.58	1.57	20.8	0.196
1.25	624	713	30.03	25.90	1.61	19.1	0.243
1.3	636	727	29.50	25.24	1.66	17.6	0.289
Sample boiled for 90 min							
1	519	598	34.48	31.18	0.5	30.9	—
1.05	554	636	33.05	29.50	1.38	27.7	0.054
1.1	569	653	32.40	28.50	1.43	25.4	0.105
1.15	592	678	31.43	27.58	1.50	22.9	0.152
1.2	614	703	30.47	26.43	1.58	20.7	0.195
1.25	626	715	29.96	25.82	1.62	19.1	0.242
1.3	640	731	29.35	25.07	1.67	17.5	0.287

work [21] an empirical formula was found for unboiled sample

$$\ln \frac{\Delta n}{W''\Delta\alpha N_c} = XD + Y \tag{20}$$

where X and Y are constants characterizing the proportionality in equation (20), Δn the birefringence, W'' the storable elastic energy of the network, $\Delta\alpha$ the optical configuration parameter and N_c the number of network chains per unit volume. By combination of the two empirical formulae we found the following relation

$$\ln \frac{\Delta n f_\theta \omega(\cos\theta)\varepsilon^{\|}}{W'' N_c \Delta\alpha\theta} = X_2 D + Y_2. \tag{21}$$

The values of X_2 and Y_2 were determined to be 8.817 and -51.108, respectively (see figure 10). From equation (21) it is clear that several parameters are affected due to thermal treatment and cold drawing processes. These changes lead to new physical characteristics for PET fibres.

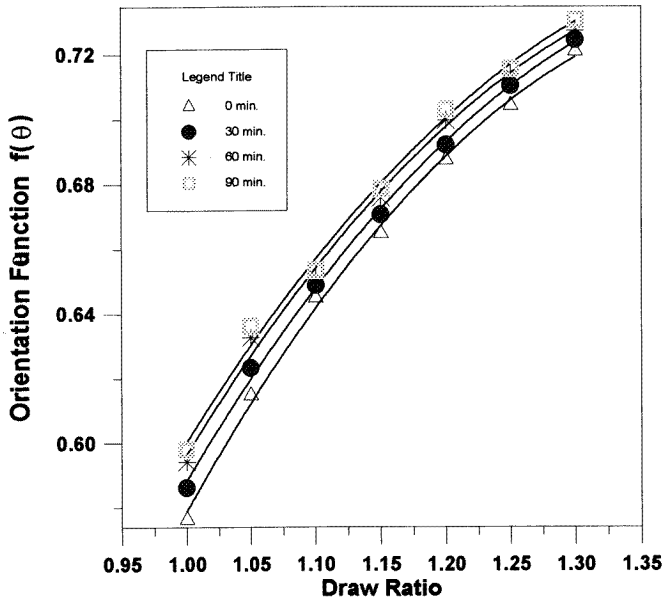

Figure 4. The relationship between the optical orientation function f_θ and draw ratio for all samples.

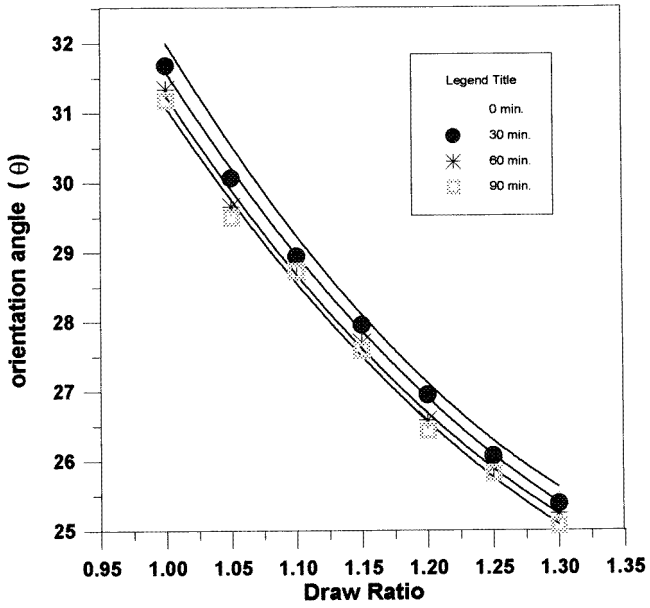

Figure 5. The relationship between the orientation angle θ and draw ratio for all samples.

4. Discussion

Deformation due to drawing processes and/or thermal treatment are the predominant means of producing new physical structure of polymeric fibres, which are so important commercially and

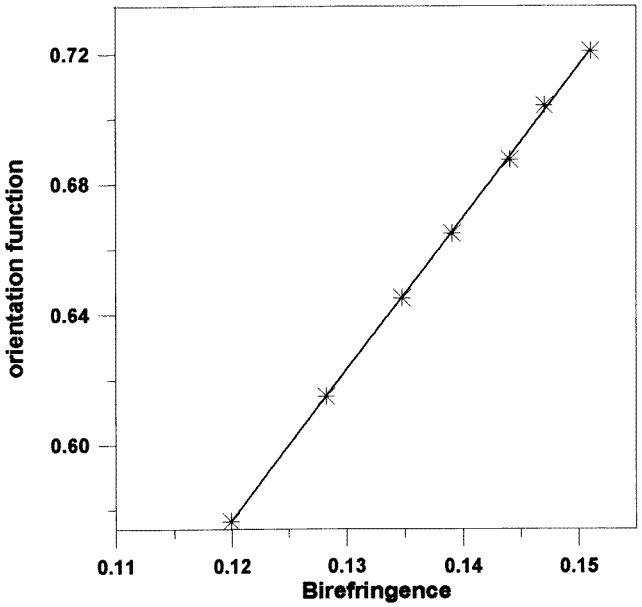

Figure 6. The relationship between the optical orientation function f_θ and the birefringence for the unboiled sample.

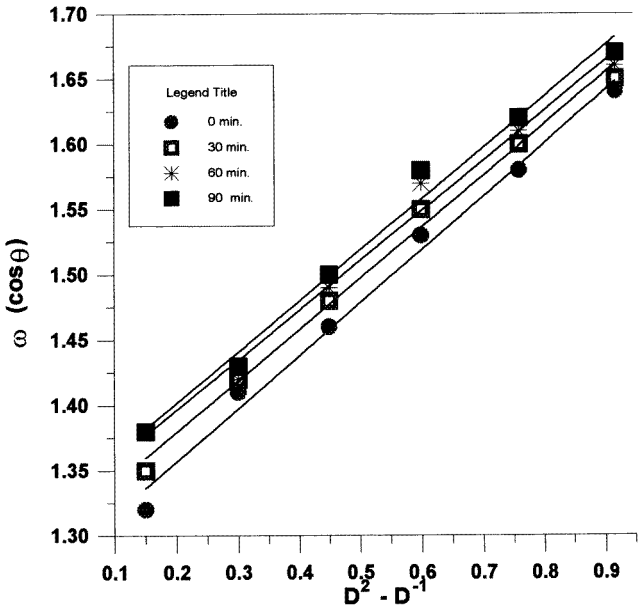

Figure 7. The relationship between $\omega(\cos\theta)$ and $(D^2 - D^{-1})$.

are of much industrial interest for man's end use. The drawing process produces reorientation at a macro-structure level when investigating mechanical properties. In addition, due to the

Table 3. Values of the polarizability of a monomer unit $\alpha^{\parallel}$, $\alpha^{\perp}$ and $\bar{\alpha}$ and the specific refractivity of the isotropic dielectric $\varepsilon^{\parallel}$, $\varepsilon^{\perp}$ and $\bar{\varepsilon}$.

D	$\alpha^{\parallel}$ $\times 10^{-36}$	$\alpha^{\perp}$ $\times 10^{-36}$	$\bar{\alpha}$ $\times 10^{-36}$	$\varepsilon^{\parallel}$ $\times 10^{-6}$	$\varepsilon^{\perp}$ $\times 10^{-6}$	$\bar{\varepsilon}$ $\times 10^{-6}$
Unboiled sample						
1	2.31	1.97	2.14	273	233	253
1.05	2.33	1.97	2.15	275	232	254
1.1	2.34	1.96	2.15	276	231	254
1.15	2.35	1.96	2.15	277	231	254
1.2	2.36	1.95	2.15	278	230	254
1.25	2.36	1.95	2.16	279	230	255
1.3	2.37	1.94	2.16	280	230	255
Sample boiled for 30 min						
1	2.32	1.97	2.15	274	233	253
1.05	2.33	1.96	2.15	276	232	254
1.1	2.34	1.96	2.15	277	231	254
1.15	2.35	1.95	2.15	278	231	254
1.2	2.36	1.95	2.16	279	230	254
1.25	2.37	1.95	2.16	280	230	255
1.3	2.37	1.94	2.16	281	230	255
Sample boiled for 60 min						
1	2.32	1.97	2.15	274	233	253
1.05	2.33	1.97	2.15	276	232	254
1.1	2.34	1.96	2.15	277	231	254
1.15	2.35	1.96	2.15	278	231	254
1.2	2.36	1.95	2.16	279	230	255
1.25	2.37	1.95	2.16	280	230	255
1.3	2.37	1.94	2.16	280	230	255
Sample boiled for 90 min						
1	2.32	1.97	2.15	274	233	254
1.05	2.34	1.96	2.15	276	232	254
1.1	2.34	1.96	2.15	277	231	254
1.15	2.35	1.95	2.15	278	231	254
1.2	2.36	1.95	2.16	279	230	255
1.25	2.37	1.94	2.16	280	230	255
1.3	2.38	1.94	2.16	280	229	255

parameters of crystallization, i.e. the chain mobility and cooling of the PET fibres, we depend on the thermal treatments to increase the mobility of the chains and the axial mobility of the microfibrils [40]. In general the thermal process changes the crystalline and amorphous parts in PET fibres, where the crystallized areas give to PET fibres high modules of rigidity, elasticity and ultimate tensile strength, whereas the amorphous areas give the fibres the flexibility, recovery, elongation and swelling.

Significant variation in the characteristic properties of PET fibres is due to the reorientation of molecules by the drawing process. Also the boiling process changes the structural behaviour due to accumulation of some structural phenomena [41]. The effect of any mechanical and thermal treatment gives knowledge for quality control in industrial processes. When a fibre is immersed in water, the water molecules infiltrate the fibre and find their way in between the long-chain molecules, hence pushing them apart. As the fibre-chain molecules are oriented in line with the axis of the fibre and as they are pushed apart, there will be a considerable increase in the diameter of the fibre [42]. The interferogram figure 1 shows irregularity along the fibres

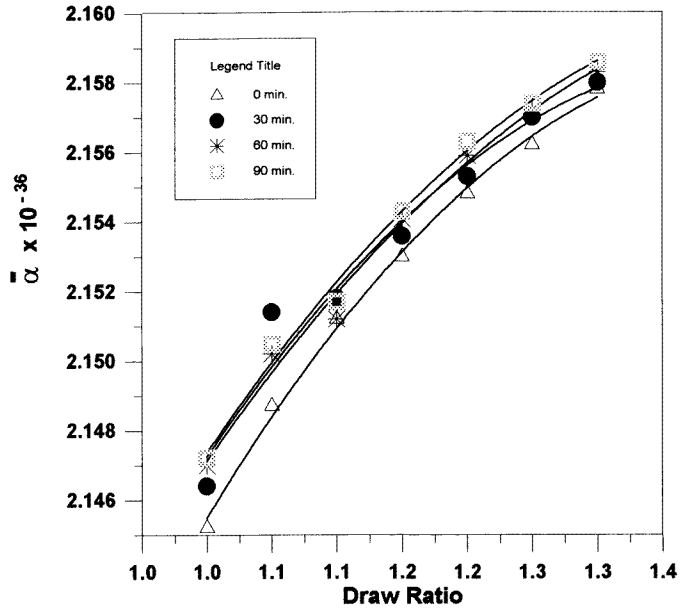

(a)

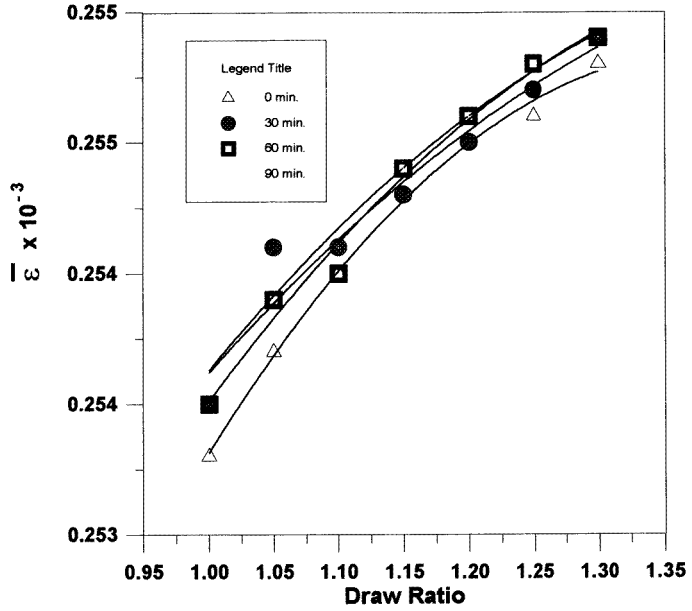

(b)

Figure 8. The relationship between the draw ratio and both the mean polarizability of a monomer unit and the mean specific refractivity of the isotropic dielectric.

axis in both the fibre diameter and fringe shift. This effect is due to the fact that the PET fibre is necked during stretching for draw ratio $1 < D \leqslant 1.3$. Calculation of the polarizability of a monomer unit $\alpha^{\parallel}$ and the specific refractivity of the isotropic dielectric $\varepsilon^{\parallel}$ in a parallel

Table 4. Values of mean square density fluctuation η^2, molar refractivity R and the number of monomer units per unit volume N_m.

D	$\eta^2 \times 10^6$	R (mol^{-1})	$N_m \times 10^{20}$
Unboiled sample			
1	29.52	89.05	42.95
1.05	29.63	89.07	42.96
1.1	29.52	89.05	42.95
1.15	29.63	89.07	42.96
1.2	29.84	89.09	42.97
1.25	29.84	89.09	42.97
1.3	29.89	89.10	42.97
Sample boiled for 30 min			
1	29.42	89.04	42.94
1.05	29.63	89.07	42.96
1.1	29.42	89.04	42.94
1.15	29.73	89.08	42.96
1.2	29.84	89.09	42.97
1.25	29.89	89.10	42.97
1.3	30.02	89.11	42.98
Sample boiled for 60 min			
1	29.73	89.08	42.96
1.05	29.73	89.08	42.96
1.1	29.84	89.09	42.97
1.15	29.89	89.10	42.97
1.2	30.02	89.11	42.98
1.25	30.08	89.13	42.98
1.3	30.02	89.11	42.98
Sample boiled for 90 min			
1	29.84	89.09	42.97
1.05	29.89	89.10	42.97
1.1	29.84	89.09	42.97
1.15	30.02	89.11	42.98
1.2	30.02	89.11	42.98
1.25	30.08	89.13	42.98
1.3	30.15	89.13	42.99

direction are found to be increased with increasing draw ratio in contrast to both $\alpha^{\perp}$ and $\varepsilon^{\perp}$ (see figures 9 and 10). This means that the series and parallel components are deformed in the same mode by drawing and thermal processes.

5. Conclusion

From the obtained values of various macro-structural parameters and their changes with the boiling and stretching the following conclusions are reported.

(1) The orientation factor and angle are found to be affected by both the drawing process and boiling time.
(2) Boiling and drawing increased the overall crystallinity and the distribution function in segments.
(3) Boiling and annealing, on the other hand, increased fibre density and this significantly also increased the chain mobility in the non-crystalline regions.

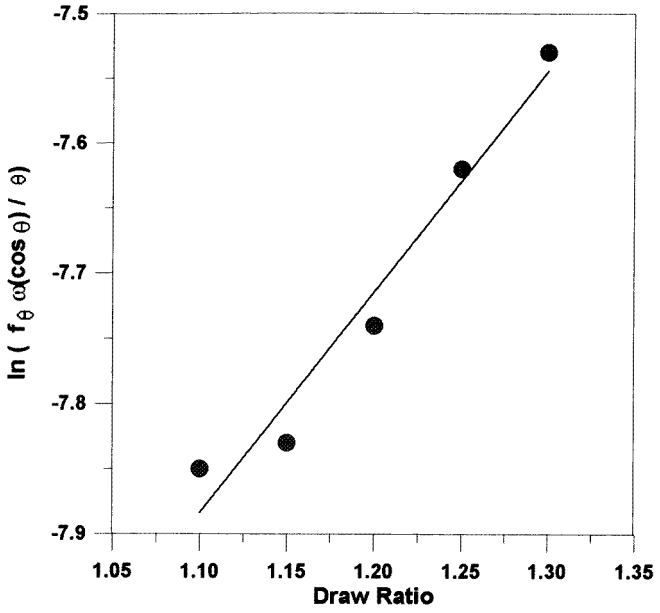

Figure 9. The relationship between ln $[f_\theta \omega(\cos\theta)/\theta)]$ and draw ratio for the unboiled sample.

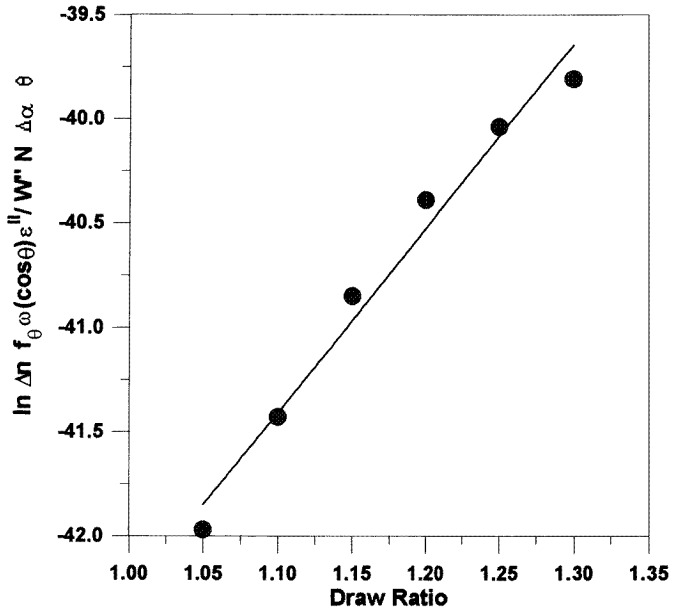

Figure 10. The relationship between $\ln[\Delta n f_\theta \omega(\cos\theta)\varepsilon^{\parallel}/W'' N_c \Delta\alpha\theta)]$ and draw ratio for the unboiled sample.

Finally, the above experimental results and calculations confirm that the drawing and boiling of PET fibres changes the physical structural parameters of such fibres and these results are useful for man's end use.

References

[1] Balmi D V, Chappel F P, Culpin M F, Madoc Joues D and Tranter T C 1961 *Rheol. Acta.* **1** 639
[2] Zbigniew K W 1977 *Formation of Synthetic Fibers* (New York: Gordon and Breach)
[3] Glenz W, Peterlin A and Wilke W 1971 *J. Polym, Sci,* A **2** 1243
[4] Hamza A A, Fouda I M, Kabeel M A, Seisa E A and El-Sharkawy F M 1998 *J. Polym. Sci.* B **36** 555
[5] Fouda I M and El-Tonsy M M 1990 *J. Mater. Sci.* **25** 121
[6] Barakat N and Hamza A A 1990 *Interferometry of Fibrous Materials* (Bristol: Hilger)
[7] Happy F 1983 *Applied Fiber Science* vol 1 (London: Academic) p 130
[8] Hamza A A, Fouda I M, Kabeel M A and Shabana H M 1996 *Polym. Testing* **15** 35
[9] Neil M A, Duckett R A and Ward I M 1988 *Polymer* **29** 54
[10] Purvis J, Boiver D I and Ward I M 1973 *Polymer* **14** 398
[11] Kashiwagi M, Cunningham A, Manual A J and Ward I M 1973 *Polymer* **14** 11
[12] Nobbs J H, Bower D I, Ward I M and Pasterson 1974 *Polymer* **15** 28
[13] Nobbs J H, Bower D I and Ward I M 1976 *Polymer* **17** 2
[14] Nobbs J H, Bower D I and Ward I M 1978 *Polymer* **19** 1100
[15] Perena J M, Duckett R A, and Ward I M 1980 *J. Appl. Polym. Sci.* **25** 1381
[16] Bower D I and Ward I M 1982 *Polymer* **23** 645
[17] Samules J R 1974 *Structured Polymer Properties* (New York: Wiley)
[18] Cunningham A, Ward I M, Willis H A and Zichy V 1974 *Polymer* **15** 749
[19] Hamza A A, El-Farhaty K A and Helaly S A 1988 *Opt. Appl.* **18** 133
[20] Fouda I M and Shabana H M *Eur. Polym. J.* at press
[21] Fouda I M and Shabana H M *Polym. Polym. Composite* at press
[22] Pluta M 1971 *Opt. Acta* **18** 661
[23] Hamza A A, Sokkar T Z N and Kabeel M A 1985 *J. Phys. D: Appl. Phys.* **18** 1773
[24] Hermans P H 1946 *Contributions to the Physics of Cellulose Fibres* (Amsterdam: North-Holland)
[25] Ward I M 1962 *Proc. Phys. Soc.* **80** 1176
[26] Ward I M 1977 *J. Polym. Sci., Polym. Symp.* **53** 9
[27] Cunningham A, Davies G R and Ward I M 1974 *Polymer* **15** 743
[28] Stein R S and Wilkes G L 1975 *Structure and Properties of Oriented Polymers* Applied Science, London p 57
[29] De Vries H 1979 *Colloid-Z. Polym. Sci.* **257** 226
[30] Hermans P H and Platzek P 1939 *Kolloid-Z.* **88** 67
[31] Kratky O 1933 *Kolloid-Z.* **64** 213
[32] Roe R J and Krigbaum W R 1964 *J. Appl. Phys.* **35**
[33] De Vries H, Bonnebat C and Beautemps J 1977 *J. Polym. Sci. Polym. Symp.* **58** 109
[34] Bourvelles G L and Beautemps J 1990 *J. Appl. Polym. Sci.* **39** 352
[35] Boder G 1991 *Structural Investigation of Polymers* ch. 7, p 326
[36] Fischer E W and Fakirov S 1976 *J. Mater. Sci.* **11** 1041
[37] Zachariodes A Z and Porter S 1983 *The Strength and Stiffness of Polymers* (New York: Dekker) p 121
[38] Jenkins A D 1972 *Polymer Science, A Material Science Hand Book* (Amsterdam: North-Holland) p 1
[39] Hemsley D A 1989 *Applied Polymer Light Microscopy* (London: Elsevier) p 7
[40] Decandi F, Vittoria V and Peterlin A 1985 *J. Polym. Sci., Polym. Phys. Edn.* **23** 1217
[41] Hamza A A, Fouda I M, Kabeel M A, Seisa E A and El-Sharkawy F M 1997 *J. Appl. Polym. Sci.* **65** 2031
[42] Moncrieff R M 1975 *Man-Made Fibers* (London: Newnes–Butterworths) p 77